# Adsorption of Cationic Dyes by Waste Biomass Treated by Phosphoric Acid

## N. Badri[*1], M. Zbair[1], A. Sahibed-Dine[1], Y. Chhiti[2], L. Khamliche[3,] and M. Bensitel[*1]

*1. Laboratory of Catalysis and Corrosion of Materials (LCCM), Department of Chemistry, Faculty of Sciences of El Jadida, University of Chouaib Doukkali, BP.20, 24000 El Jadida, Morocco.*
*2. Science Engineer Laboratory for Energy (LabSIPE), National School of Applied Sciences, Chouaïb Doukkali University, El Jadida, Morocco*
*3.Chemistry Department, laboratoire de chimie bio-organiques, Faculty of Science, 24000 El Jadida, University of Chouaib Doukkali, Morocco.*

**Abstract**
This work investigated the capacity of the Moroccan Date Pits (TMDP) (treated by phosphoric acid) to adsorb Methylene Blue (MB) from aqueous solution. The performance of TMDP was characterized by proximate analysis, $N_2$ adsorption-desorption isotherms, SEM, XRD and FTIR. The equilibrium studies are carried out under a large range of MB concentration (from 60 to 400 mg/L) using 200 mg of the adsorbent at room temperature and pH 8. The efficiency of the adsorption tests are evaluated by the Langmuir and Freundlich isotherm models. Equilibrium data fitted well by Langmuir model with a maximum of the adsorption capacity of 106 mg/g, equivalent to 99% of removal. The pseudo-second-order model described better the adsorption process. TMDP has shown promising results for MB adsorption. This material will be tested for other industrial dyes in our future works.

## 1. Introduction

Organic micropollutants as pharmaceutical compounds, endocrine upsetting compounds, pesticides, industrial dyes and others are available in the environment. Without any structural intervention, the amount of these pollutants is expected to grow constantly in the next decades. This worries both scientists and regulatory offices. The vast majority of these compounds are not yet identified. Their effect mechanisms on aquatic flora, animals and human are not well known. Along these lines, enhanced techniques for examination have distinguished these micropollutants at lower concentrations ($\mu g\ L^{-1}$ to $ng\ L^{-1}$). Methylene blue (MB) is considered a compound marker for surface water pollution because of it is routinely used during the process in the textile industry and produces a lot of wastewater volumes [1]. Therefore, effluents derived from textile and dye activities can cause a severe environmental impact on water bodies of neighboring receptors due to the presence of toxic reactive dyes [2]. In recent years, the adsorption techniques have demonstrated a simple and cost-effective knowledge in terms of energy requirements and environmental friendliness to expel dyes from industrial wastewater, and has attracted the attention of researchers. Adsorption technique in textile dyes removal is widely investigated. using different wastes biomass are tested as adsorbent giving good performance [3,4]. For example, wheat straw has presented presents high removal efficiency of cationic dyes such as methylene blue, methyl violet and crystal violet [5–7] and heavy metals [8].

The target of this research is to evaluate the performance of Moroccan Treated Date Pits to adsorb the methylene blue discharged through the textile industry waste to an expanded concentration range. This Date Pit is considered as one of the best candidate among the agriculture wastes, after being treated, due to its low-cost, quite availability and high carbon content. For this purpose, MDP is chemically treated using phosphoric acid and then pyrolyzed at 400°C. Some objects of this work are : to study the feasibility of using TMDP as an adsorbent for removal MB dye; to determine the characterisation of TMDP; to determine the applicability of various isotherm models (Langmuir and Freundlich ) based on the correlation coefficient to find out the best-fit isotherm equation; to determine the adsorption mechanism between MB and TMDP.

## 2. Material and Methods

### 2.1. Methylene Blue solutions

The solution was prepared by dissolving 1 g of Methylene Blue (MB) (Sigma Aldrich) in 1 L of distilled water. From the concentrated solution, six diluted solutions with various concentrations (60, 80, 100, 200, 300 and 400 mg/L) were prepared.

### 2.2. preparation of the adsorbent

The Moroccan Date Pits was collected from Ouarzazate region in Morocco. Raw material was washed with hot distilled water to remove impurities and then dried and crushed to low particle size (about 200 µm).

The impregnation process is performed by respecting ratio of MMDP / $MH_3PO_4$=1/2. After impregnation, the sample was pyrolyzed under purified nitrogen at 400 °C for 1 h. Finally, the sample is washed several times and dried at 80°C. The prepared sample was labeled TMDP.

### 2.3. Batch Adsorption Studies

Batch adsorption was studied to determine the removal efficiency of MB from different aqueous solution concentrations (from 60 to 400mg/L). 0.2 g of TMDP is added 100 ml of a MB solution. Samples were kept at room temperature and agitated at 200 rpm for 3 h to reach the equilibrium. Then, the samples were filtered to separate TMDP from the MB and minimize interferences. The amount of MB remained in the solution after absorption is determined by Ultraviolet-Visible (UV-Vis) spectrophotometry analysis at 664,5nm.

The adsorption capacity, Qe;t (mg/g), is calculated through the relationship:[9-10].

$$Q_{e;t} = \frac{(C_0 - C_{e;t})}{m} * V \quad (1)$$

Where

$C_0$ (mg/L) is the initial concentration of MB;

$C_{e;t}$ (mg/L) is the concentration of MB at equilibrium time ;

$V$ (L) is the volume of the solution;

$m$ (g) is the mass of the TMDP;

$Q_{e;t\ (mg/g)}$ is the adsorption capacity at equilibrium time.

### 2.4. Characterization of prepared adsorbents

The use of these adsorbent supports in the field of water treatment requires knowledge of their physicochemical properties. The characterization parameters helps to explain the phenomena that govern the efficiency and the adsorption capacity of the TMDP used.

The proximate analysis allowed to determine the product distribution (moisture, volatile matter, fixed carbon and ash) obtained after MDP heat treatment under specified conditions.

### 2.4.1. Proximate analysis

Pore size distribution, surface area and pore volume of TMDP were measured by nitrogen adsorption/desorption using a micrometrics analyzer.

### 2.4.2. Scanning Electron Microscopy (SEM)

Morphological characterizations of MDP and TMDP were performed using Scanning Electron Microscopy (SEM) Hitachi S 3400 N.

### 2.4.3. FTIR analysis

Fourier Transform Infrared (FTIR) analysis was used to detect the available functional groups on the TMDP and MDP surface. Infrared spectra were recorded on a FTIR 8400S, Shimadzu with samples prepared as KBr disks on the 400-4000 cm$^{-1}$ range.

### 2.4.4. X-Ray Diffraction (XRD) analysis

X-ray diffraction (XRD) analysis was used to identify the nature of the crystalline and amorphous phases present in a solid. However, several crystalline meshes must follow one another to form lines [11].

X-ray diffraction powder patterns were obtained on a D8 Advance diffractometer using Cu Ka radiation source ($Λ$= 1.5418Å).

# 3. Results and discussion

## 3.1. Characterization results

The proximate analysis of MDP and TMDP samples are presented in Table 1. TMDP contain a significant percentage of fixed carbon (about 50%) which is due to the previous considerable removal of volatiles mater during the treatment phase.

**Table1:** Proximate analysis of MDP and TMDP

| Samples | Volatile matter (%) | Ash content (%) | Moisture content (%) | Fixed carbon (%) |
|---------|---------------------|------------------|----------------------|-------------------|
| **MDP** | 60.20 | 0.99 | 10 | 28.81 |
| **TMDP** | 42 | 0.10 | 7.59 | 50.31 |

According to the literature, there are six types of adsorption isotherm [12]. As showed in Figure 1(a) TMDP present adsorption isotherm of type I/IV according to IUPAC (International Union of Pure and Applied Chemistry) with a type $H_4$ hysteresis which is associated with capillary condensation suggest that the sample is mainly mesoporous and contain a small number of micropores. The initial part of the type IV isotherm is attributed to monolayer-multilayer adsorption. The BET surface area ($S_{BET}$) and pore volume (V) of TMDP is 852 $m^2.g^{-1}$ and 0.42 $cm^3.g^{-1}$ respectively. The pore size distribution of TMDP was calculated in the standard manner by using Barret-Joyner-Halenda (BJH) method. As shown in Figure 1(b), there are several sharp peaks appearing at a small pore area (micropores area) about 5-15 Å.
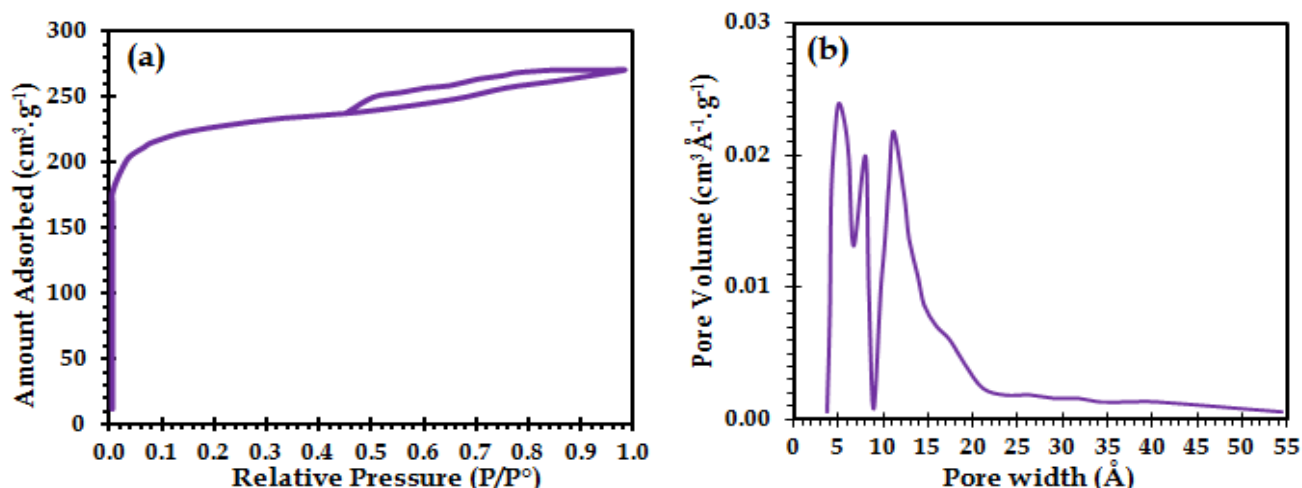


**Figure 1: (a)** adsorption-desorption isotherm **(b)** BJH pore size distribution of TMDP

The characterization of surface MDP and TMDP was performed by Scanning electron microscope (SEM) the SEM images is shows in figures 2(a) and 2(b) revealed a significant changes on surface morphology of MDP after treatment. MDP has undergone both chemical and thermal treatment. Therefore, TMDP showed high porosity compared to MDP. Indeed, the impregnation with phosphoric acid followed by pyrolysis dehydrated the cellulose material, resulting in weakening of the precursor structure and creation of pores. Phosphoric acid is responsible for decomposition of organic material. This facilitates the release of volatile matter during pyrolysis process and consequently the development of the porositie [13].

Infrared spectroscopy was used in this study to evaluate the modifications in the chemical nature of MDP after treatment. The Infrared spectroscopy spectra shown in **Figure 3** that the majority of bands are disappeared after treatment of MDP, except the wide band located in the range of 3200–3400 $cm^{-1}$ that is a consequence of O-H groups and adsorbed water molecules [14] and the band at 1623 $cm^{-1}$ which characterizes the bending of water molecules [15]. This is explained by the disappearance of most functional groups during the pyrolysis treatment. The assignment of the main functional groups of MDP is shown in **Table 2**.
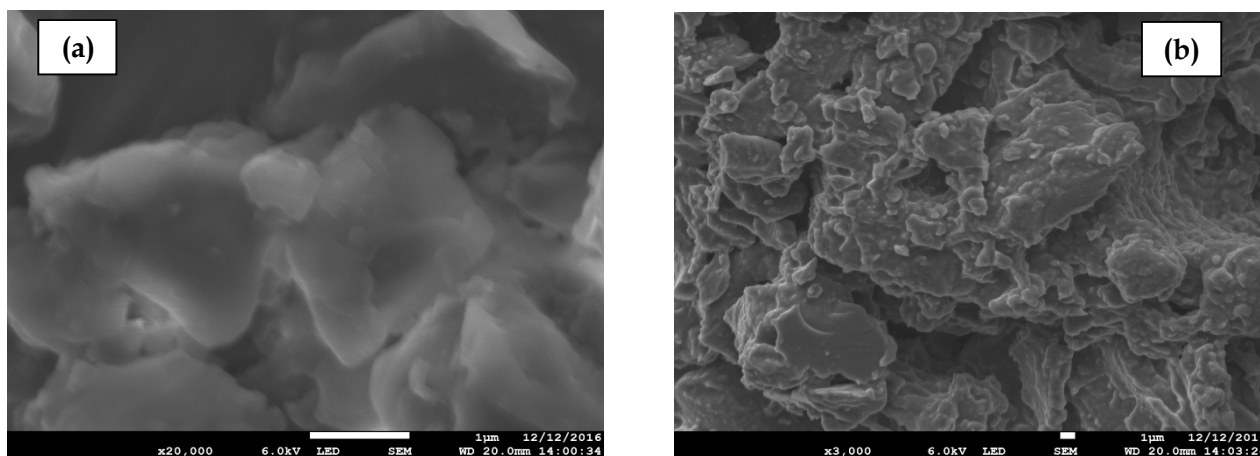
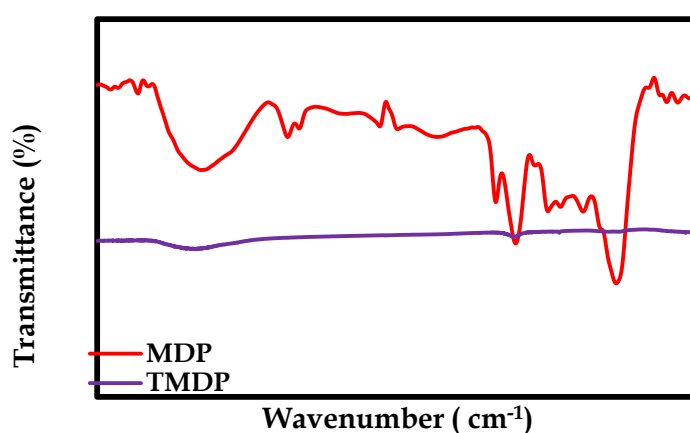**Figure 2: (a)** Scanning electron micrographs of (MDP, **(b)** TMDP)



**Figure 3:** FTIR spectrum of MDP and TMDP

**Table 2:** Appropriation of main functional groups of MDP

| Wavenumber (cm$^{-1}$) | Functional group |
|---|---|
| 2913-2844 | CH stretching of CH2 and CH3 groups |
| 1737 | C=O stretching of acetyl or carboxylic acid |
| 1482 | CH2 bending |
| 1232 | C-O stretching of ether linkage |
| 1045 | C-O symmetric stretching of primary alcohol |
| 700-400 | C-C stretching (lignin) |

X-ray diffraction model of TMDP (**Figure 4**) shows a broad peaks at 2θ = 24° corresponding to the reflection of the (002) plane. This reveals an amorphous nature of material, which is advantageous for well-defined adsorbent [16].

### 3.2. Effect of contact time and initial concentration on MB adsorption

**Figure 5** exhibits the impact of contact time and initial concentration on MB removal by TMDP. The results showed that the amount of adsorbate fixed on the material increases with the increase in the content of the solution in blue of methylene. In fact, the increase in concentration induces an increase in the driving force of the concentration gradient, thus increasing the diffusion of the dye molecules in solution through the surface of the adsorbent [17]. Evenly, the adsorption increase rapidly with increasing concentrations of MB. After this period, the equilibrium reached. The adsorption capacity at equilibrium (*Qe*) increased from 29.60 to 177.87 mg/g when initial concentration was increased from 60 to 400 mg/L. At equilibrium, more than 83% of the MB was adsorbed into TMDP. Over time, the pore sites became occupied by MB molecules and adsorption decreased [18].
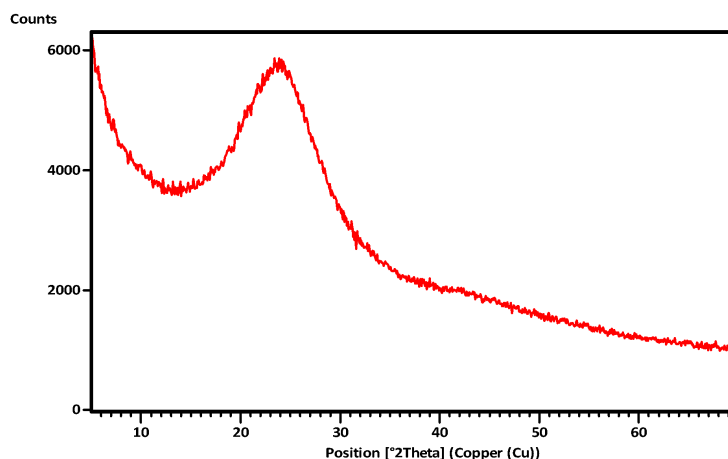
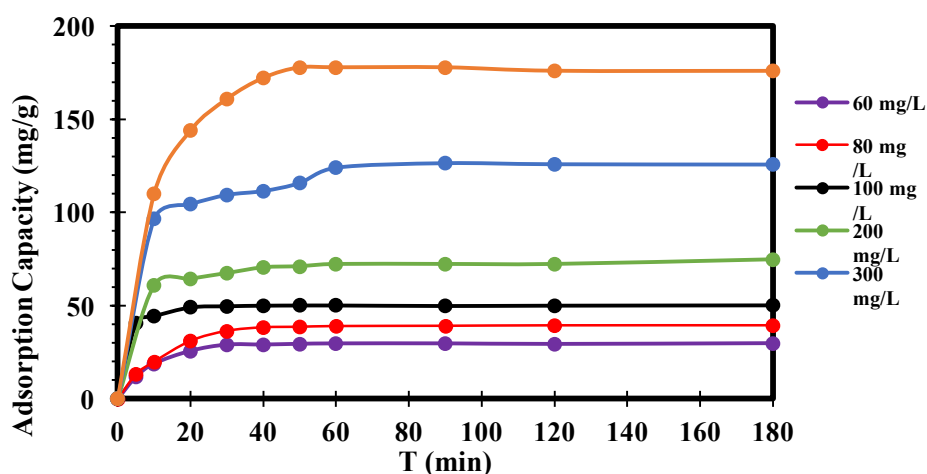**Figure 4:** X-ray diffraction model of TMDP



**Figure 5:** Effects of contact time on the adsorption capacity at different initial MB concentrations (TMDP: T=25°C, TMDP mass= 200 mg, pH= 8)

*4. Kinetic Modeling*

To investigate the kinetics of MB adsorption onto TMDP, adsorption constants were determined by using both pseudo-first-order and pseudo-second-order models [19] (**Table 3**).

**Table 3:** Appropriation of main functional groups of MDP

| Kinetic models | Equation | Description | References |
|---|---|---|---|
| Pseudo-First-Order | $(Q_e - Q_t) = Q_e - K_1$ | Qt= Adsorbed amount at time t, Qe= Adsorbed amount at equilibrium, K1= rate constant ; | [19] |
| Pseudo-Second- Order | $\dfrac{1}{Q_t} = \dfrac{1}{K_2 \, Q_e^2} + \dfrac{1}{Q_e}$ | K2= rate constant | [19] |

Figure 6 (a) and 6 (b) present the first and the second order kinetic models respectively. The adsorption kinetics were better explained with the pseudo-second-order model. **Table 4** presents the experimental and theoretical adsorption capacities with the rate constants at different MB concentrations. Moreover, $R^2$ quantifies the accuracy of correlation. The R² values for all concentrations are close to 1 indicate a perfect correlation between the theoretical and the experimental results. The R² values are lower for the first-order kinetic model for the most MB concentrations. Indeed, this model is not the appropriate to describe the adsorption process. However, the process follows pseudo second order kinetics. These observations lead us to say that the adsorption of methylene blue does not express a controlled diffusion process since it does not follow the pseudo-first order equation given by Lagergren [20].

Table 4 also shows that the rate constant $k_2$ decreases from 0.010 to 0.002g/mg.min. At lower concentrations, BM dye ions existent in the adsorption medium could interact with the binding sites, hence higher rate constant results. At elevated concentrations, because of the saturation of the adsorption sites, the rate constant of dye adsorption shows a decreasing trend. This is due to the remaining vacant surface sites being difficult to occupy due to repulsive forces between the dyes molecules on the adsorbent surface [21].
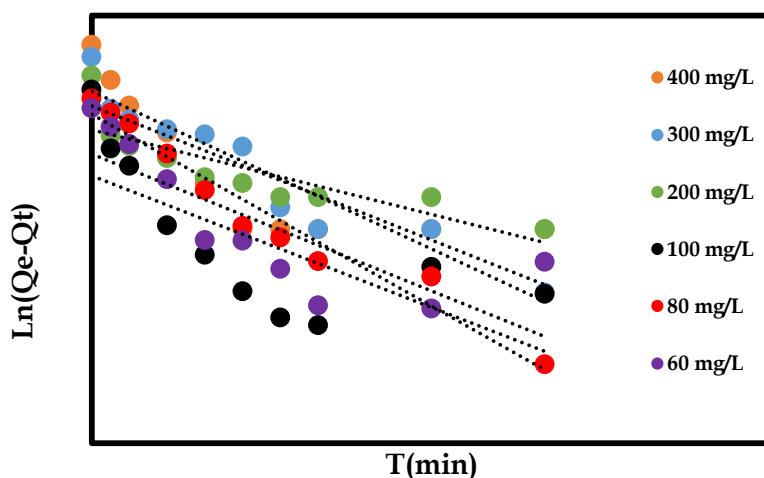


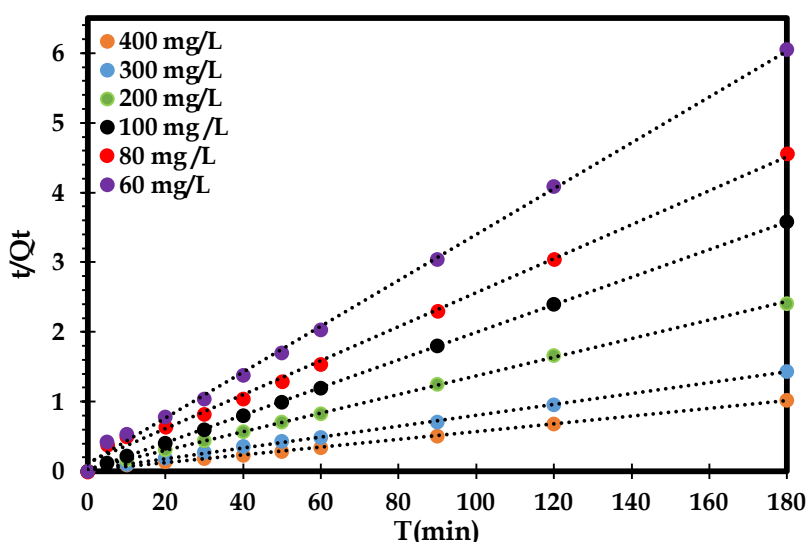**Figure 6 (a):** Pseudo-first-order kinetics for MB adsorption onto TMDP



**Figure 6 (b):** Pseudo-second-order kinetics for MB adsorption onto TMDP

**Table 4:** Pseudo-first-order and second-order rate constants at different initial concentrations of MB adsorption onto TMDP

| $C_0$ (mg/L) | Qe,exp | Pseudo-First-Order | | | Pseudo-Second-Order | | |
|---|---|---|---|---|---|---|---|
| | | Qe,cal (mg/g) | $K_1$ (min-1) | $R_2$ | Qe,cal (mg/g) | $K_2$ (g/mg.min) | $R_2$ |
| 60 | 29.60 | 8.33 | 0.098 | 0.6455 | 30.39 | 0,010 | 0.9983 |
| 80 | 39.02 | 25.42 | 0.137 | 0.9540 | 40.98 | 0.005 | 0.9965 |
| 100 | 50.22 | 4.46 | 0.094 | 0.5117 | 50.50 | 0.034 | 0.9999 |
| 200 | 72.22 | 16.40 | 0.060 | 0.7186 | 75.18 | 0.005 | 0.9994 |
| 300 | 124.14 | 48.54 | 0.113 | 0.9118 | 128.20 | 0.002 | 0.9983 |
| 400 | 177.87 | 31.82 | 0.096 | 0.6408 | 178.57 | 0.002 | 0.9986 |

### 4.1. Adsorption Isotherms

Different models were used to investigate the interaction between adsorbate and adsorbent at equilibrium. Among these, the Langmuir and Freundlich isotherms are the most appropriate models used in the literature [21]. According to the Langmuir isotherm, adsorption occurs at homogenous sites and forms a monolayer. It

means that once adsorbate is attached to a site, no further adsorption can take place. Freundlich isotherm is used for modeling the adsorption on heterogeneous surfaces [22]. The linear form of Langmuir and Freundlich isotherms equations are given in **Table 5** [23, 24].

**Table 5:** Isotherm models**.**

| Isotherm | Equation | Description | References |
|---|---|---|---|
| **Langmuir** | $$\frac{1}{Q_e} = \frac{1}{(K_L Q_{max})\,C_e} + \frac{1}{Q_{max}}$$ | $C_e$: concentration at equilibrium; $Q_e$ = adsorption capacity in equilibrium; $Q_{max}$ = maximum adsorption capacity; $K_L$= langmuir constant | [23] |
| **Freundlich** | $$ln\,Q_e = \frac{1}{n}ln\,C_e + ln\,K_F$$ | $K_F$= Freundlich constant; n = adsorption intensity; 1/n = 0 irreversible; 1/n>unfavourable 0 <1/n< 1 favourable | [24] |

**Table 6** shows the values of the correlation coefficient ($R^2$), $Q_{max}$ and $K_L$ were calculated from the plot in **Figure 7** using the least squares method. For the Langmuir isotherm, the $R^2$ is 0,9194, reflecting a favorable adsorption of MB onto TMDP. The value of $Q_{max}$ is 106 mg/g suggesting a very strong monolayer adsorption to the surface. The value of $R_L$ is 0,015 L/g indicating a favorable sorption energy. The Freundlich isotherm, assumes that adsorption takes place on heterogeneous sites and forms a multilayer with different distributions of energy levels [24].

The $K_F$ is 28, 01 and the n is 2,670. The high value of *n* indicates favorable adsorption conditions for MB in aqueous solution. The $R^2$ for the adsorption MB is 0,876, slightly less than Langmuir isotherm and consequently a less favorable adsorption.
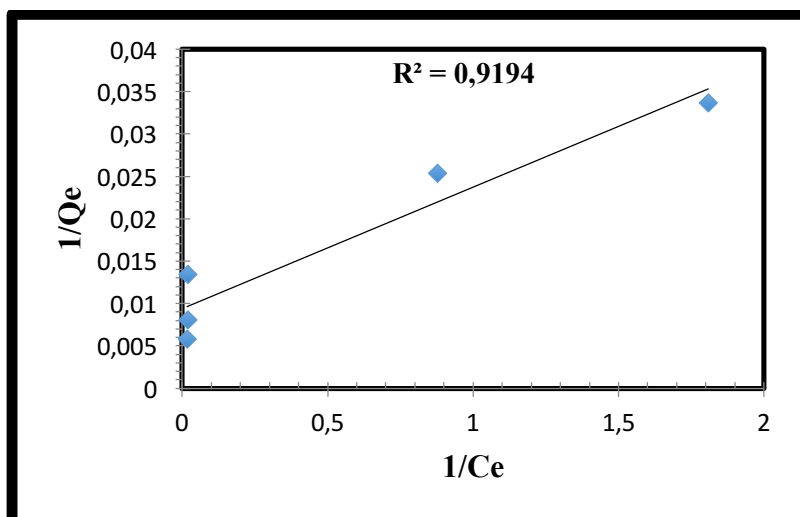


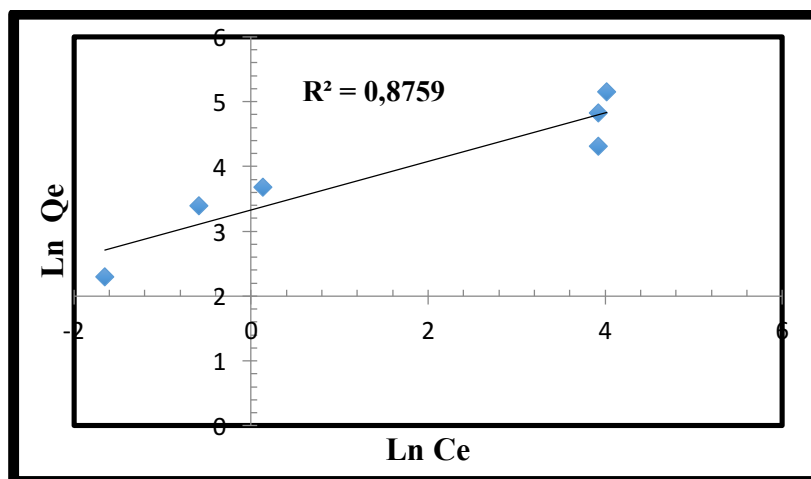**Figure 7:** Langmuir isotherms for MB adsorption onto TMDP.



**Figure 8:** Freundlich isotherms for MB adsorption onto TMDP. Not cited

**Table 6:** Isotherm parameter constants for MB adsorption onto TMDP.

| Langmuir | | | Freundlich | | |
|---|---|---|---|---|---|
| $Q_{max}$ (mg/g) | $R_L$ (L.min$^{-1}$) | $R^2$ | $K_F$ (mg/g) | n | $R^2$ |
| 106,00 | 0,015 | 0,9194 | 28,01 | 2,670 | 0,8759 |

### 4.2. Intra-particle diffusion study

The diffusion mechanism cannot identify either by the pseudo-first-order or by the pseudo-second-order kinetic model. The intraparticle diffusion varies with the square root of time is given by (Weber and Morris, 1963) [25].
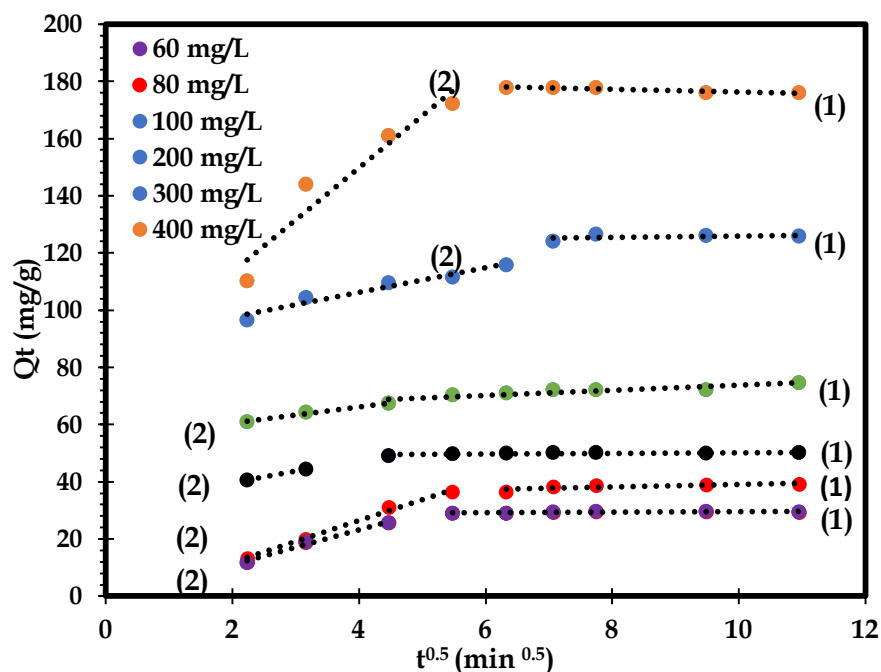


**Figure 9:** Intra particle diffusion plot for adsorption of MB on TMDP for different initial MB concentrations

Figure 9 shows that the plots are not linear over the whole time range that confirms more than one process affect the MB dye adsorption. The plot show two slops of straight lines (**Figure 9**). The first line is linear, representing macropore and mesopore diffusion and the second depicting micropore diffusion. Furthermore, the second line region corresponds to the intra-particle pore diffusion in which methylene blue diffuse throughout the porous surface of the TMDP [25-26].

## Conclusion

The adsorption of MB from aqueous solution was investigated under different experimental conditions in batch process using treated waste biomass (TMDP). The different adsorption capacities of the active carbons studied show that the BM adsorbs preferentially in the mesopores that are accessible to these molecules.
The Langmuir adsorption isotherm has the best fit to the experimental data with a maximum adsorption capacity of 106 mg/g indicating a very strong monolayer adsorption to the surface. In addition, the data showed that the second-order equation provide the best correlation for the experimental data which indicate the chemical sorption process. The results of this study indicated that TMDP, a low-cost adsorbent, have a good performance and could be used as an alternative to commercial-activated carbon for wastewater treatments.

## References

1. B.R Babu, A K Parande, S Raghu, T.P Kumar, Cotton Textile Processing : Waste Generation and Effluent Treatment, J. Cotton Sci. 153 (2007) 141–153.
2. a S Daba, O.U Ezeronye, Bioremediation of textile effluent using Phanerochaete chrysosporium, African J. Biotechnol. 4 (2005) 1548–1553.
3. S Rangabhashiyam, N Anu, N Selvaraju, Sequestration of dye from textile industry wastewater using agricultural waste products as adsorbents, J. Environ. Chem. Eng. 1 (2013) 629–641.

4. B.H Hameed, Removal of cationic dye from aqueous solution using jackfruit peel as non-conventional low-cost adsorbent, J. Hazard. Mater. 162 (2009) 344–350.

5. V.M Vučurović, R.N Razmovski, U.D Miljić, V.S Puškaš, Removal of cationic and anionic azo dyes from aqueous solutions by adsorption on maize stem tissue, J. Taiwan Inst. Chem. Eng. 45 (2014) 1700–1708.

6. L Zhou, B Huang, He Zhang, H Li, Peach gum for efficient removal of methylene blue and methyl violet dyes from aqueous solution, Carbohydr. Polym. 101 (2014) 574–581.

7. F.A Pavan, E.S Camacho, E.C Lima, G.L Dotto, V.T.A Branco, S.L.P Dias, Formosa papaya seed powder (FPSP): Preparation, characterization and application as an alternative adsorbent for the removal of crystal violet from aqueous phase, J. Environ. Chem. Eng. 2 (2014) 230–238.

8. V.B.H Dang, H.D Doan, T Dang-Vu, A Lohi , Equilibrium and kinetics of biosorption of cadmium(II) and copper(II) ions by wheat straw, Bioresour. Technol. 100 (2009) 211–219.

9. M.Z ALAM, S.A MUYIBI, M.F MANSOR, R WAHID, Activated carbons derived from oil palm empty-fruit bunches: Application to environmental problems, J. Environ. Sci. 19 (2007) 103–108.

10. A.T Mohd Din, B.H Hameed, A.L Ahmad, Batch adsorption of phenol onto physiochemical-activated coconut shell, J. Hazard. Mater. 161 (2009) 1522–1529.

11. M Molina-Sabio, F Rodriguez-Reinoso, Caturla F., Sellès M.J.. Mise au point de porosité d'activation de dioxyde de carbone acide phosphorique combiné. Carbone, 34 (1996) 457-462.

12. Hill de Boer, the Dynamical character of adsorption, 2nd Edition, Clarendon Press, Oxford,UK, (1968).

13. R Malik, D.S Ramteke, S.R Wate, Adsorption of malachite green on groundnut shell waste based powdered activated carbon, Waste Manag. 27 (2007) 1129–1138.

14. Y Guo, D.A Rockstraw, Physicochemical properties of carbons prepared from pecan shell by phosphoric acid activation, Bioresour. Technol. 98 (2007) 1513–1521.

15. A.C Lua, T Yang, Characteristics of activated carbon prepared from pistachio-nut shell by zinc chloride activation under nitrogen and vacuum conditions, J. Colloid Interface Sci. 290 (2005) 505–513.

16. W Tongpoothorn, M Sriuttha, P Homchan, S Chanthai, C Ruangviriyachai, Preparation of activated carbon derived from Jatropha curcas fruit shell by simple thermo-chemical activation and characterization of their physico-chemical properties, Chem. Eng. Res. Des. 89 (2011) 335–340.

17. N Fayoud, S Alami Younssi, S Tahiri, A Albizane, Kinetic and thermodynamic study of the adsorption of methylene blue on wood ash (Kinetic and thermodynamic study of the adsorption of methylene blue on wood ashes), J. Mater. Environ. Sci. 6 (11) (2015) 3295-3306.

18. I.A.W Tan, A.L Ahmad, B.H Hameed, Adsorption isotherms, kinetics, thermodynamics and desorption studies of 2,4,6-trichlorophenol on oil palm empty fruit bunch-based activated carbon, J. Hazard. Mater. 164 (2009) 473–482.

19. N.K Amin, Removal of reactive dye from aqueous solutions by adsorption onto activat carbons prepared from sugarcane bagasse pith, Desalination. 223 (2008) 152–161.

20. H Qiuhong, X Zhiping, Q Shizhang, F Haghsereht, G Michael Wilson, L Qing, Une nouvelle élimination de la couleur adsorbant de hétérocoagulation cationiques et anioniques argiles, J.Colloïde. Entre. Sci., 308 (2007) 191-199.

21. C Meziti, A Boukerroui, removal of a basic textile dye from aqueous solution by adsorption on regenerated clay, Procedia Engineering 33 (2012) 303 – 312.

22. B.H Hameed, I.A.W Tan, A.L Ahmad, Adsorption isotherm, kinetic modeling and mechanism of 2,4,6-trichlorophenol on coconut husk-based activated carbon, Chem. Eng. J. 144 (2008) 235–244.

23. I Langmuir, the Constitution and Fundamental Properties of Solids and Liquids. Part I. Solids., J. Am. Chem. Soc. 252 (1916) 2221–2295.

24. H.M.F Freundlich, Over the adsorption in solution, J. Phys. Chem. 57 (1906) 385–471.

25. K Arvind, J Hara Mohan, Adsorption of Cr(VI) from aqueous phase by highsurface area activate carbon prepared by chemicalactivation with $ZnCl_2$, Process Safety and Environmental Protection 109 (2017) 61-73.

26. O.S Bello, Adsorptive removal of malachite green with activated carbon prepared from oil palm fruit fibre by KOH activation and $CO_2$ gasification, South African J. Chem. 66 (2013) 32– 41.

(2018) ; http://www.jmaterenvironsci.com